Distribution Category
UC-66

LAWRENCE LIVERMORE LABORATORY
University of California/Livermore, California/94550

UCRL-52699

IMPERIAL VALLEY ENVIRONMENTAL PROJECT: AIR QUALITY ASSESSMENT

D. L. Ermak, R. A. Nyholm, and
P. H. Gudiksen

MS. date: April 4, 1979

DISCLAIMER

CONTENTS

IMPERIAL VALLEY ENVIRONMENTAL PROJECT: AIR QUALITY ASSESSMENT

ABSTRACT

This report is an assessment of the potential impact on air quality of geothermal development in California's Imperial Valley. The assessment is based on the predictions of numerical atmospheric transport models. Emission rates derived from analyses of the composition of geothermal fluids in the region and meteorological data taken at six locations in the valley over a 1-yr period were used as input to the models. Scenarios based on 3000 MW, 2000 MW, 500 MW, and 100 MW of power production are considered. Hydrogen sulfide is the emission of major concern. Our calculations predict that at the 3000-MW level (with no abatement), the California 1-h standard for H_2S(42 $\mu g/m^3$) would be violated at least 1% of the time over an area of approximately 1500 km^2 (about 1/3 of the valley area). The calculations indicate that an H_2S emission rate below 0.8 g/s per 100-MW unit is needed to avoid violations of the standard beyond a distance of 1 km from the source. Emissions of ammonia, carbon dioxide, mercury, and radon are not expected to produce significant ground level concentrations, nor is the atmospheric conversion of hydrogen sulfide to sulfur dioxide expected to result in significant SO_2 levels.

INTRODUCTION

This report presents an assessment of the potential impact on air quality of emissions from geothermal power plants to be located in the Imperial Valley, California. Development of Imperial Valley geothermal resources is in the initial stages; the first 50-MW power plants are expected to come on-line within the next year. Over the next 20 to 30 years, the level of energy production is expected to grow to several thousand megawatts of electrical capacity.

Geothermal resources are generally exploited by building small (50–150 MW) power units sequentially rather than by developing the whole field at once. After a number of years, with the approach of full field development, maximum electrical capacity is reached. The impact of a single unit is usually evaluated before construction begins; however, such studies do not present a clear picture of the impact of full field development. The purpose of this study is to assess the impact of large-scale development on air quality so that if mitigation measures are needed, they can be planned for prior to development.

Geothermal power plants release several gaseous substances to the atmosphere, including carbon dioxide, hydrogen sulfide, ammonia, mercury, and radon. The principal gas constituent of geothermal fluids (after water) is CO_2, but CO_2 emissions are not expected to have any negative environmental impact. The main emission of concern is H_2S, which is a nuisance because of its noxious odor.

The concentration level of each species emitted will ultimately depend on: the concentration of the gas in the geothermal fluid, the efficiency and type of energy conversion technology, the amount of abatement, the number and location of the power plants, and the regional meteorology. For purposes of this study, data on gas concentrations in the geothermal fluid have been obtained from several geothermal wells in the Imperial Valley. The gas emission rate per power plant has been calculated on the basis of an assumed energy conversion efficiency consistent with the temperature of the geothermal fluid. No reduction in the emission rate as a result of abatement

controls is assumed. Thus, the analysis should give conservative results, leading to an estimate of the level of emission control that is necessary.

We assume a total production of 3000 MW, generated by thirty 100-MW power units spread throughout the valley. This production level is well within current estimates of the maximum capacity of the resource. Regional analyses for each of the four Known Geothermal Resource Areas (KGRA) in the valley are described in the Appendix. These can be combined to evaluate the effects of different regional capacities and emission rates. For example, a 2000-MW scenario is addressed, assuming that 500 MW are produced in each KGRA, with equal emission rates. We have also evaluated a single 100-MW power plant to more clearly address the question of localized impacts.

The air quality assessment is based on the predictions of numerical atmospheric transport models. In addition to emissions data, the major input to these models is meteorological data, obtained from continuous monitoring over a 1-yr period at six locations within the valley. The models predict the average concentration level of each emitted species over the entire region. Averaging times were varied from 1 h to as long as 1 yr, depending on the concentration standard applicable to that species.

ATMOSPHERIC TRANSPORT MODELS

The primary model used in this study is ATMAS,[1] which numerically solves the three-dimensional advection-diffusion equation for atmospheric transport. In this model, the advection term represents the average wind velocity, and the diffusion term represents eddy diffusion due to turbulence in the atmosphere. ATMAS generates a three-dimensional, time-varying wind field from average wind velocity data taken at several locations within the region of interest. Eddy diffusion is assumed to occur in a Gaussian manner, with the dispersion rate (σ_y) calculated from the measured variation in the wind direction (σ_θ).

The computer code uses the particle-in-cell concept[2-4] to solve the advection-diffusion equation. This method relies upon a large number of marker particles (10,000 to 20,000) to represent the mass distribution of the emitted species within a three-dimensional Eulerian grid. The concentration of the particles is defined at the cell centers using a weighted sum of the surrounding particles. The locations of the marker particles are defined by their individual coordinates within the Eulerian grid. The marker particles are transported through the grid with a pseudo-velocity derived from the transport equation and defined at the cell corners. In a typical time cycle, each marker particle in a given cell is transported for one time step with the velocity obtained from a weighted sum of the pseudo-velocities at the eight corners of the cell. This permits a new set of particle coordinates to be computed and results in a new concentration distribution. In source regions, marker particles are continually injected into the grid at a rate consistent with the source strength.

ATMAS is designed to assess the long-term air quality impacts of continuous emissions from multiple area sources. The code is a simplified and computationally faster version of the transport code ADPIC.[5] Its speed is due primarily to the use of flat terrain, a coarser advection grid, and the assumption of Gaussian diffusion. It does, however, retain the important effects of a time and spatially varying wind velocity and wind shear. Extensive validation of the ADPIC code has been performed against closed solutions of the advection-diffusion equation and against numerous tracer experiments out to a distance of about 100 km. Since ATMAS is based on the same model equations as ADPIC and has also been validated against closed solutions of the advection-diffusion equation, we feel that it has been adequately verified.

The principal output of ATMAS is a time sequence of hourly averaged ground-level concentrations on a two-dimensional grid of the region. There is a separate sequence for each species studied. These data are analyzed to determine longer averages (e.g. monthly or yearly), the probability of exceeding a given threshold or standard, and other statistical descriptions. Regional data are presented in the form of contour plots, while data for a single location are presented in the form of histograms, graphs, and bar plots.

A minimum simulation period of 1 yr was desired to provide predictions of air quality levels in

future years. Although ATMAS is computationally much faster than more complex versions of the code, it still requires considerable computer time (approximately 4 h on a CDC 7600 to simulate one month). Consequently, ATMAS was used to simulate only one month in each season (April, July, October, and January, 1977-78). The assessment of the remaining months was based on the results of the atmospheric transport model MSDM.[6]

The MSDM code solves the atmospheric advection-diffusion equation using the steady-state assumption, which results in a Gaussian plume type model. The wind field is assumed to be constant for each case so that the effects of spatial variations in the wind field are neglected. The principal meteorological data required by the code are atmospheric stability, wind speed, and wind direction. The MSDM code can operate in either a climatological or instantaneous mode. The climatological mode calculates average concentrations over periods of months to years using a joint frequency distribution to describe the probability of meteorological conditions; the instantaneous mode calculates average concentrations for periods of minutes to hours for a specific set of meteorological conditions. The meteorological data used in these calculations were obtained from the meteorological station closest to each source.

As a check to ensure that these simplifications did not lead to erroneous results, the MSDM code was also run for the four months in which ATMAS was used, and the results of the two codes were then compared. The agreement was found to be quite good. In regions of high concentration, the values were generally within a factor of 1.5 of each other. On a regional scale, the isopleth contour plots of the average concentration were found to be in very good agreement.

The main output of MSDM when run in either the climatological or instantaneous mode is a regional plot of ground-level concentration contours resulting from the combined emissions of all sources considered. The impact of individual sources is also analyzed. Typical output for single-source calculations includes the plume center-line and average concentration, the probability of exceeding short-term standards as a function of downwind distance from the source, and contour plots of the average concentration.

METEOROLOGICAL AND AMBIENT AIR QUALITY DATA

The meteorological and baseline air quality data were obtained from six fixed-location monitoring stations shown in Fig. 1. These stations were operated from December 1976 to April 1978, and detailed descriptions of the data are given by Gudiksen[7] and Gudiksen *et al.*[8] The primary meteorological parameters used in the atmospheric transport calculations are wind velocity, atmospheric stability, and temperature inversion height. A full year of data was used in this study, with the sampling period extending from February 1, 1977 to January 31, 1978.

The Imperial Valley lies within the zone of prevailing westerlies and on the east side of the semipermanent high pressure area of the northeast Pacific Ocean. Consequently, the prevailing flow over the valley is from the west during most of the year. This is shown in Fig. 2 by the yearly averaged wind roses for each of the station locations. During the summer, a significant southeasterly component occurs as a result of intense surface heating, which produces a thermal low-pressure region over the valley. Histograms of the average wind speed at a

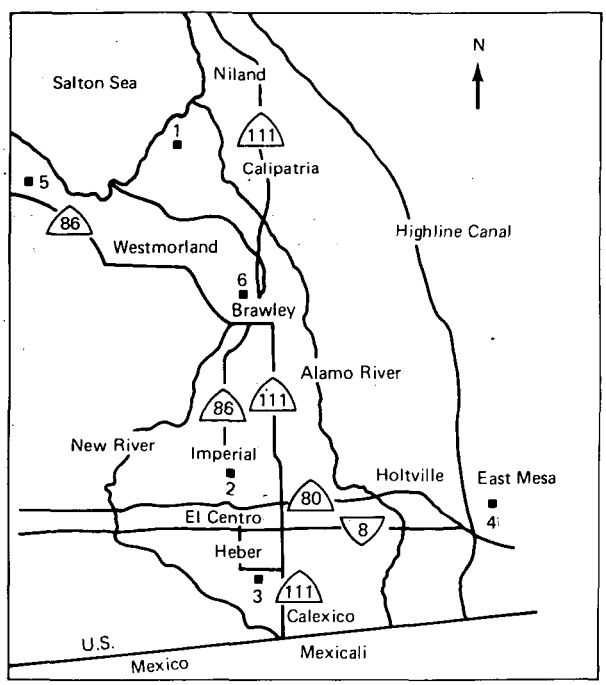

FIG. 1. Locations of the six air quality monitoring stations in the Imperial Valley, California.

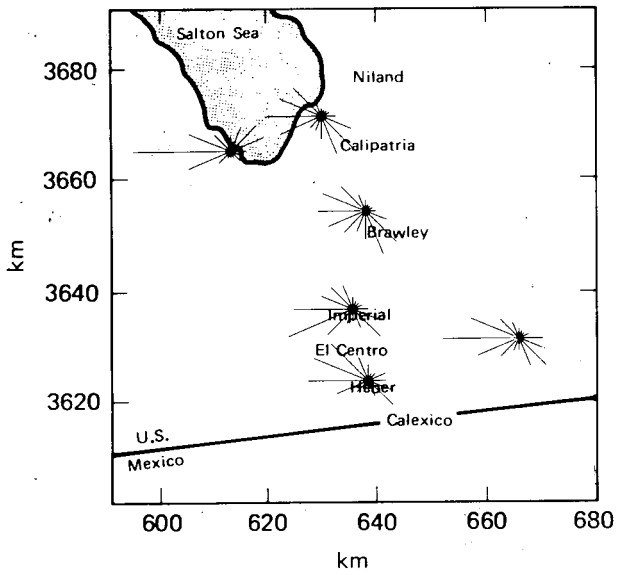

FIG. 2. Wind roses of the yearly averaged frequency distribution of wind direction in the Imperial Valley, California. The bar points in the direction from which the wind is blowing, and its length (80 km = 100%) represents its frequency of occurrence in percent. The coordinates used in this and subsequent figures are Universal Transverse Mercator (UTM) coordinates.

height of 10 m are given in Fig. 3. The median wind speed ranged from 2.3 to 3.1 m/s, depending on the location.

Atmospheric stability was estimated from measurements of the standard deviation of the horizontal wind direction fluctuation σ_θ at a height of 10 m above the ground surface at the Heber station. The σ_θ values were used to determine the standard Pasquill–Gifford stability categories. A histogram of the yearly averaged probability of each class is shown in Fig. 4. Stable conditions (categories F and E) are seen to be the dominant condition, with the less stable E category occurring a bit more often. In the winter, the situation is reversed from the yearly average, and category F occurs more often.

Temperature inversion heights were measured with an acoustic sounder located at the Brawley station. The data reveal a diurnal pattern that persisted throughout the year. A surface-based temperature inversion occurred regularly at night, and typically, by mid-morning it had disappeared or risen above the 1-km range of the instrument. The reverse process occurred during the early evening hours, with reformation of the surface-based inversion again at night.

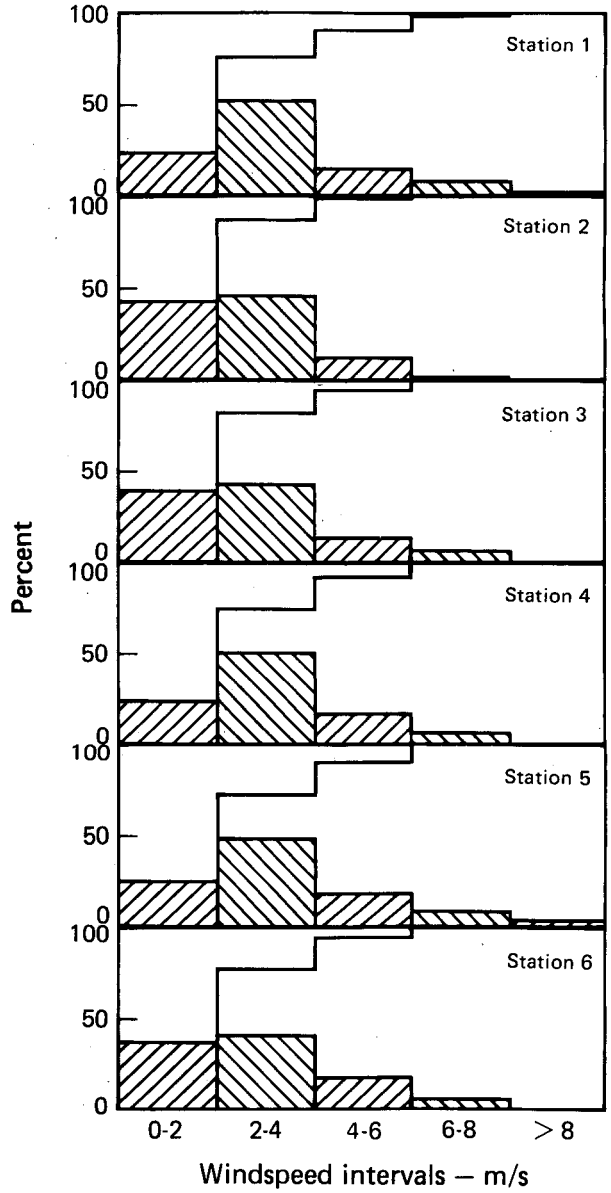

FIG. 3. Yearly histograms of wind speed when averaged on 15-min intervals for each of the six air quality stations given in Fig. 1.

The gas concentration levels calculated by the atmospheric transport models are due solely to the postulated geothermal sources and do not consider contributions from other sources. However, baseline measurements made at the six meteorology stations can be used to estimate the contribution from all other sources. The major species of concern from a geothermal development viewpoint is hydrogen sulfide. Also considered are sulfur dioxide, which can be formed by the atmospheric oxidation of hydrogen sulfide, and carbon dioxide, which is the major gas emission from a geothermal power plant.

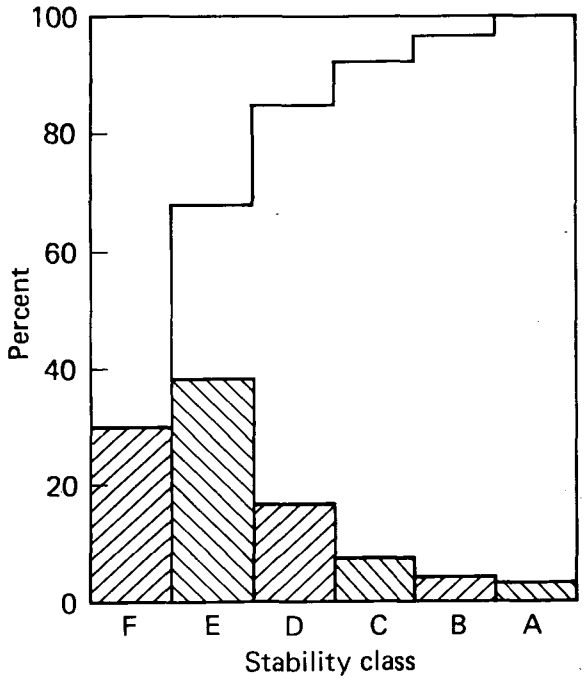

FIG. 4. Yearly histogram of atmospheric stability for Imperial Valley, California. Stability categories F to A, respectively, correspond to the σ_θ intervals: 0–3.8, 3.8–7.6, 7.6–12.6, 12.6–17.6, 17.6–22.6, and above 22.6 degrees.

The ambient concentrations of hydrogen sulfide and sulfur dioxide were low throughout the valley. Histograms of the 1-h average concentrations are shown in Fig. 5, where the results from all stations have been combined.

With the exception of a few periodic excursions, hydrogen sulfide values are less than 15 $\mu g/m^3$. The excursions appear to occur randomly throughout the year and may be due, at least in part, to nearby agricultural fertilizing operations. The extreme values range between 85 and 110 $\mu g/m^3$, except at the East Mesa station, where the maximum values rarely exceeded 42 $\mu g/m^3$, the California 1-h standard.

The sulfur dioxide concentrations are generally below 50 $\mu g/m^3$, with occasional excursions above this value. The Heber station recorded somewhat higher concentrations than the other stations, probably because of its proximity to the principal population centers in the valley. However, even the maximum values are significantly below the Federal SO_2 air quality standard of 1310 $\mu g/m^3$.

Carbon dioxide concentrations were found to vary widely throughout the valley. The six-station average was 640 mg/m^3, with a standard deviation of about 65 mg/m^3.

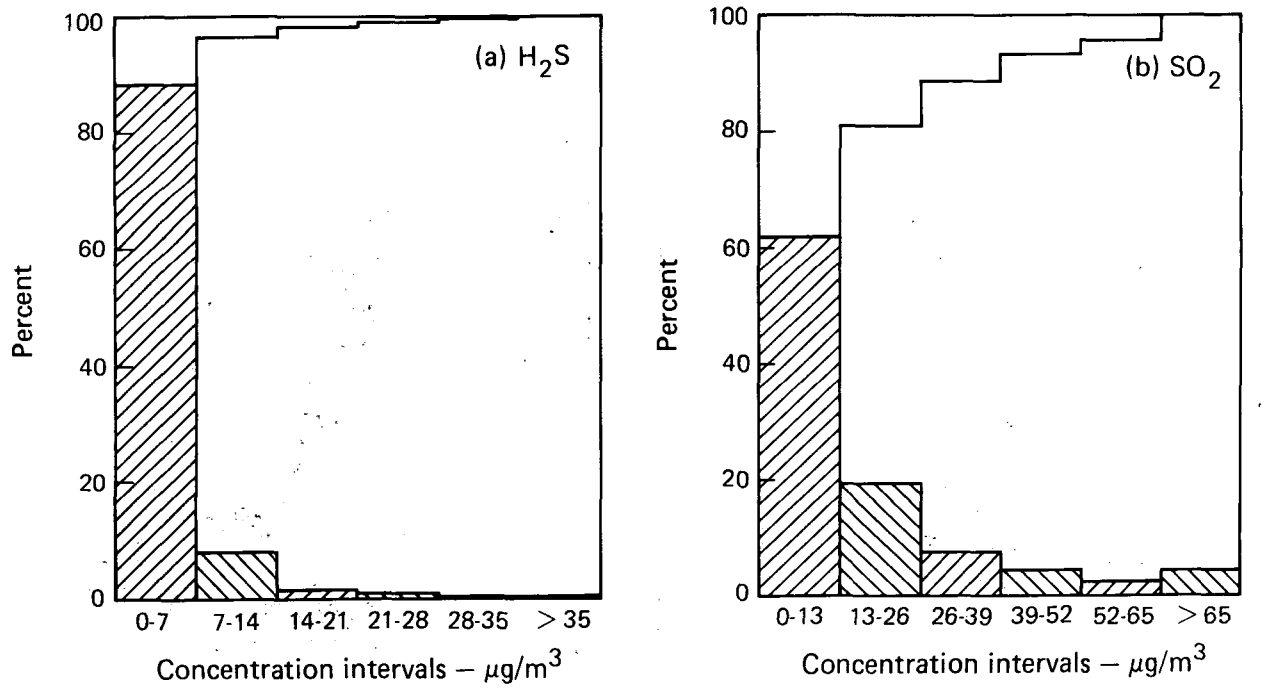

FIG. 5. Yearly histograms of the ambient baseline concentrations of H_2S and SO_2.

EMISSION INVENTORY

Within the Imperial Valley, four separate areas have been identified by the U.S. Geological Survey as Known Geothermal Resource Areas (KGRAs). Shown in Fig. 6, these areas are referred to as the Salton Sea, Brawley, Heber, and East Mesa KGRAs. It is estimated that the total resource is capable of supporting 3000 to 5000 MW of continuous electrical power production over a 30-year period.[9-10] Estimates indicate that most of the resource (possibly as much as 60%) is within the Salton Sea KGRA. However, this KGRA may be difficult to develop because the geothermal fluids have a high total dissolved solids content and about half the resource is beneath the Salton Sea.

The main power level to be assessed in this study is 3000 MW. This level represents the maximum capacity for full-field development in a medium-growth estimate for the valley.[11] The medium-growth scenario projects that electrical capacity first comes on-line in the early 1980s and then increases at a rate of about 100 MW per year until the year 2010, when the 3000-MW level is reached. This level is maintained through 2020 and then decreases linearly to zero by 2050. The scenario requires a total electrical energy production equivalent to 4000 MW of continuous power for 30 years and is therefore well within current estimates of the resource size. It is assumed that the 3000 MW is produced by 30 power plant units each with a 100-MW average output. The units are distributed as follows: 14 in the Salton Sea KGRA, 6 in the Brawley KGRA, 7 in the Heber KGRA, and 3 in the East Mesa KGRA. The siting pattern for each cluster of units is shown in Fig. 7.

The emission rate of a particular gas will depend on the concentration of that gas in the geothermal fluid, the rate of geothermal fluid consumption, and the fraction of the gas released from the power plant. The fraction of the gas released will vary depending on the type of geothermal technology used (e.g., flashed-steam, binary, or confined-flow) and the efficiency of the abatement system if one is used. For the purposes of this study, it is assumed that all gas entering the power plant is released to the atmosphere. This situation most closely approximates a flashed-steam process in which the gases are vented to the atmosphere with no abatement.

The concentration of the gases of interest in the geothermal fluid (H_2S, NH_3, CO_2, Hg, and Rn) was measured by investigators from Battelle Pacific Northwest Laboratories[12] and from LLL. Samples

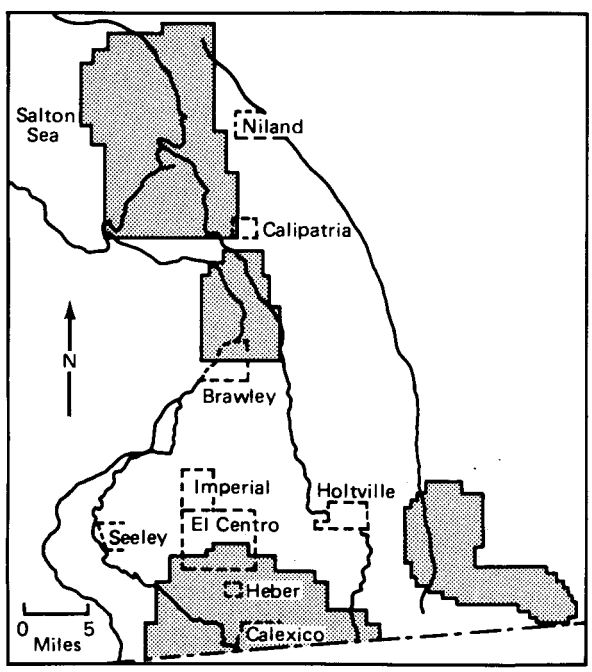

FIG. 6. Known Geothermal Resource Areas of the Imperial Valley, California.

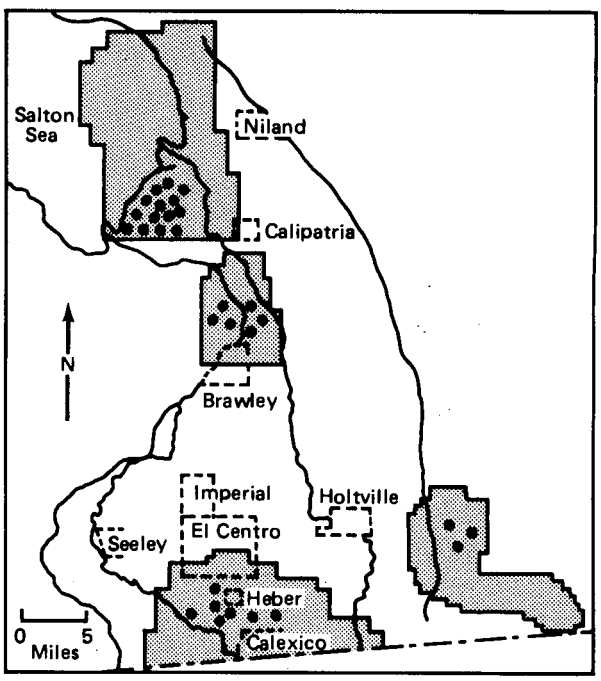

FIG. 7. Siting pattern for the 30 power plant units in the 3000-MW scenario.

were obtained from a number of geothermal wells in the Salton Sea and East Mesa KGRAs. Investigators were unable to obtain access to the other areas. The data reveal that even in wells within the same KGRA, the concentration of a specific gas may vary over an order of magnitude.

The rate of fluid consumption in geothermal power production is largely a function of the temperature of the geothermal fluids. The geothermal fluids in the Salton Sea and Brawley KGRAs have a higher temperature and therefore will be consumed at a lower rate than the fluids in the Heber and East Mesa KGRAs. On the basis of the physical and chemical characteristics of the geothermal fluids and the current designs of proposed flashed-steam power plants, approximately 50 kg of fluid from the Salton Sea and Brawley KGRAs are required per kWh of generated power, while twice as much fluid is needed to produce the same output in the Heber and East Mesa KGRAs.[13-16] Using these consumption rates and the average concentration of each gas in the geothermal fluid, we obtained the emission rates shown in Table 1. The emission rates for the Brawley KGRA are taken to be the same as the Salton Sea rates, and the Heber emission rates are taken to be the same as the East Mesa rates.

As mentioned above, each power plant unit has an output of 100 MW. The emission source from each unit is approximated in the computer calculations by a Gaussian-shaped source with a horizontal standard deviation of 20 m, a vertical standard deviation of 10 m, and a center height of 30 m. These dimensions are approximately the size of a typical cooling tower source. In the ATMAS calculations, the emission source from each cluster of power plant units is combined into a quasi-area source that is uniform in the horizontal direction, Gaussian in the vertical direction (with a standard deviation of 10 m), and elevated to a center height of 30 m.

TABLE 1. Estimated emission rates for geothermal power plants in the Salton Sea and East Mesa Known Geothermal Resource Areas (KGRA).

	Salton Sea KGRA			East Mesa KGRA		
	Concentrations, mg/kg of fluid		Emissions,	Concentrations, mg/kg of fluid		Emissions,
	Range	Mean	g/MWh	Range	Mean	g/MWh
H_2S	1.6-6.0	3.2	160	0.12-1.6	0.54	55
NH_3	20-41	35	1750	1.3-8.1	4.5	455
CO_2	1100-3800	1700	8.5×10^4	270-2300	1100	1.1×10^5
CH_4	3.0-10	6.0	300	4.0-56	33	3.3×10^3
Hg	0.0016-0.002	0.0018	0.090	0.005-0.007	0.0064	0.6
Rn	540-1080[a]	810[a]	4.1×10^4	420-540[a]	480[a]	4.9×10^4

[a]pCi/kg of fluid.

MODEL RESULTS: 3000-MW SCENARIO

HYDROGEN SULFIDE

An isopleth plot of the annual average H_2S concentrations throughout the valley is given in Fig. 8. The concentration contour levels run from 1 to 30 $\mu g/m^3$. As would be expected, the higher levels are found in the areas surrounding the power plant clusters. The highest levels are in the area of the Salton Sea KGRA, where a maximum average concentration of about 34 $\mu g/m^3$ occurs. The average level in the Salton Sea area is about five times as great as that in the Heber and East Mesa areas. This is due to the large number of power plants located in the Salton Sea KGRA and also to a higher emission rate per power plant for this area. The contours surrounding the Brawley and Salton Sea power plant clusters merge due to their proximity.

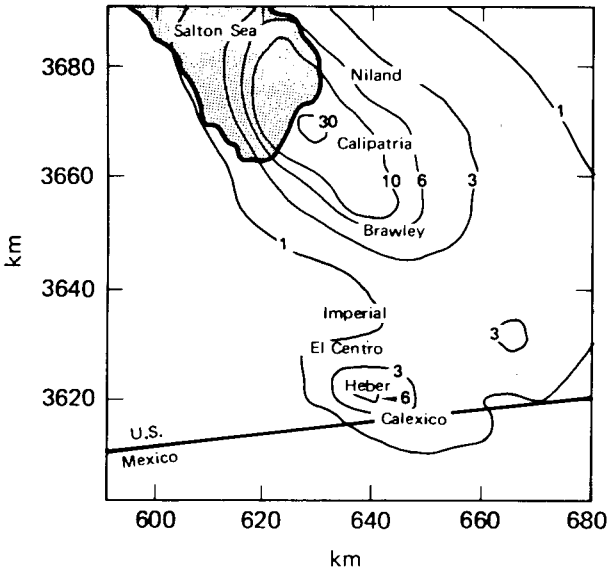

FIG. 8. Isopleth plot of the annual average ground level H_2S concentration in $\mu g/m^3$.

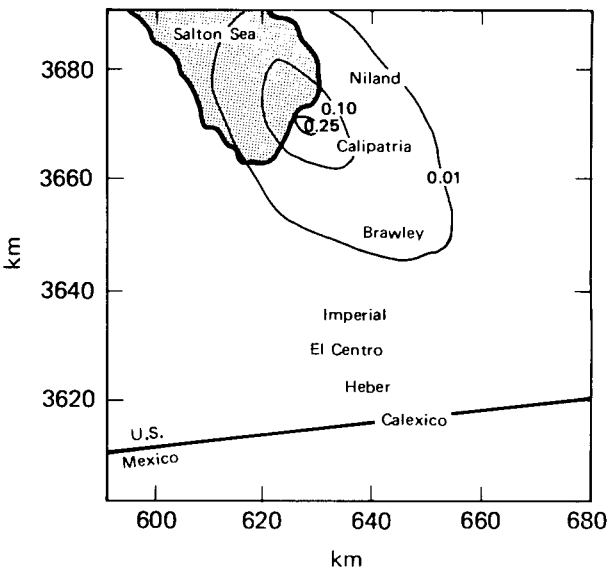

FIG. 9. Isopleth plot of the probability that the H_2S ground level concentrations will exceed the 42-$\mu g/m^3$ California 1-h-average air quality standard.

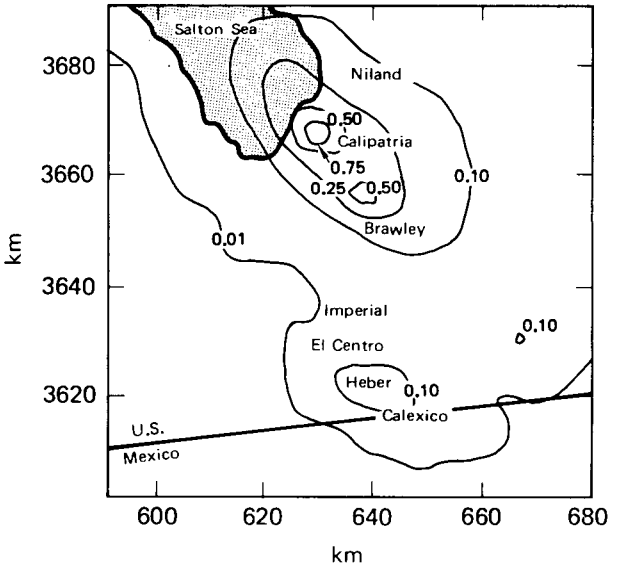

FIG. 10. Isopleth plot of the probability that the H_2S ground level concentrations will exceed the 10-$\mu g/m^3$ 1-h-average level.

The noxious odor of H_2S is the main concern, and, therefore, the short-term average concentration is of major importance. We have calculated the probability that the 1-h average H_2S concentrations will exceed 42 $\mu g/m^3$ and 10 $\mu g/m^3$ in the Imperial Valley. The higher level is the California ambient air quality standard for 1-h averages of H_2S. The lower level is approximately that at which a majority of people can detect the odor.[17]

The results for the California standard are shown in Fig. 9 in the form of a contour plot of probability levels. The 1% contour encloses an area of about 1500 km^2 surrounding the Salton Sea and Brawley power plants. In the vicinity of the Salton Sea power plants, the H_2S standard is exceeded about 25% of the time. Figure 10 shows the results for the 10-$\mu g/m^3$ level. In this case, the 1% contour covers most of the valley. In the vicinity of the power plants, the probability of exceeding the 10-$\mu g/m^3$ level is about 10% for East Mesa, 15–20% for Heber, 50% for Brawley, and 75% for the Salton Sea.

Another approach that gives insight into expected H_2S levels is to calculate histograms for single points to show the probability that H_2S concentrations will be within certain limits. As shown in Fig. 11, 22 points were chosen throughout the valley, including the centers of most cities and a number of points in Mexico and the outer regions of the valley. The results are shown in Fig. 12. The points with the largest probability of exceeding the California standard lie within the Brawley–Salton Sea area (points 13, 14, and 15) as expected. The cities of Niland (1), Calipatria (2), Westmorland (3), and Brawley (4) exceed the standard from about 2 to 10% of the time. The results at points 16, 17, and 18 indicate that, for the 3000-MW scenario, H_2S levels above 42 $\mu g/m^3$ should not extend far into Mexico as a result of Imperial Valley geothermal plants.

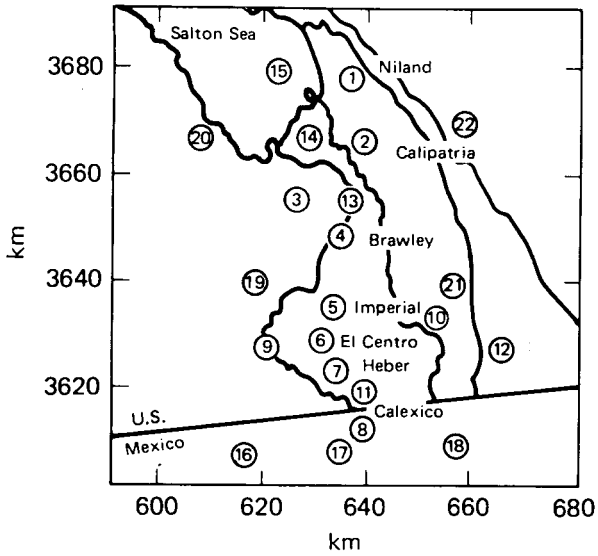

FIG. 11. The locations of the 22 analysis sites used in evaluating the probability that H_2S concentrations will be within certain limits.

Associated with each histogram are two numbers. The top one is the calculated number of days per year with at least one breach of the California standard. (The days referred to are calendar days.) The lower number is the calculated average number of hours per day in which such episodes occur. As shown in histograms 1 through 4, the northern cities in the valley experience episodes of greater than 42 $\mu g/m^3$ from 72 to 228 days per year for an average of 2 to 3 h per day. This is a very significant fraction of the year, and episodes appear to occur throughout the year. The cities in the Heber and East Mesa areas—Heber (7), Calexico (11), and Holtville (10)—have episodes on about 14 days per year. Mexicali was calculated to have three 1-h episodes, but this number is too small to be statistically meaningful. There were no calculated episodes exceeding the 42-$\mu g/m^3$ level in the cities of Imperial and El Centro.

SULFUR DIOXIDE

In these calculations, it is assumed that sulfur dioxide is produced by chemical transformation of hydrogen sulfide in the atmosphere. To approximate this, the models use first-order chemical transformation of H_2S to SO_2 with a half-life of 13 h. The resulting annual average SO_2 concentration is shown in Fig. 13. Compared to the federal standard for an annual average (80 $\mu g/m^3$), the values forecast for the valley are quite low. The maximum level (7.4 $\mu g/m^3$) occurs over the Salton Sea.

In addition to the annual SO_2 standard, there are standards for shorter periods of time in both California and federal regulations. The California SO_2 standards are more stringent, so they will be considered here.

The California 24-h standard is 105 $\mu g/m^3$, and the 1-h standard is 1310 $\mu g/m^3$. Our calculations indicate that neither of these standards would be violated under a 3000-MW scenario. In the areas where SO_2 levels were expected to be highest, the calculated 1-h-average SO_2 concentration was below 5 $\mu g/m^3$ at least 80% of the time. A few excursions into the 100-to-400-$\mu g/m^3$ region were observed, but even these maximum levels are far below the 1-h standard. Calculations of the 24-h average showed only a few episodes into the 40-to-90-$\mu g/m^3$ region.

OTHER EMISSIONS

The impact of ammonia, mercury, and radon emissions was found to be insignificant. The federal ammonia standard is 3.5 $\mu g/m^3$ (approximately the odor threshold), and the maximum ammonia concentration calculated throughout the valley was more than a factor of 10 below that level. The federal occupational standard for mercury is 100 $\mu g/m^3$, and the maximum level calculated throughout the valley was more than a factor of 200 below that. The federal standard for radon and its short-lived daughters in unrestricted areas is 10^3 pCi/m^3. The maximum level calculated in the valley was more than 5 orders of magnitude below the standard.

Carbon dioxide is the major gaseous emission from geothermal power plants, and one might expect that it could have a beneficial impact on the surrounding agricultural industry by increasing crop growth rates. Air quality measurements taken throughout the valley indicate that the average baseline CO_2 level is 640 mg/m^3 with a standard deviation of $\pm 10\%$. The maximum calculated values for this scenario were less than 100 mg/m^3, and typical values were less than 20 mg/m^3. Thus, the increase in the CO_2 level due to geothermal energy production is expected to be within the range of natural ambient fluctuations in this region.

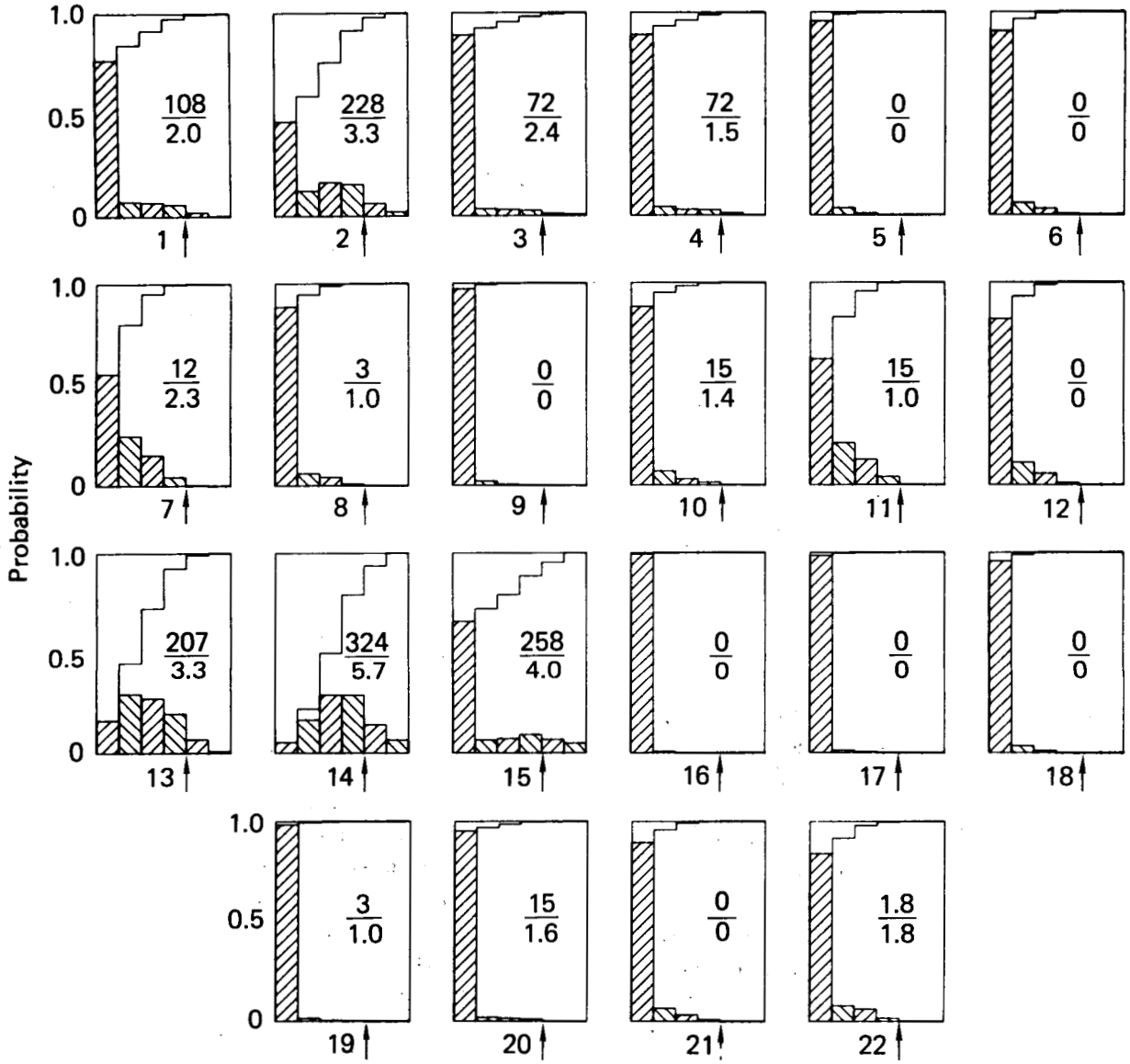

FIG. 12. Probability histograms of the hourly ground-level H_2S concentrations for the 22 sites shown in Fig. 11. Bars 1 through 6 (numbered from left to right) give results for the concentration intervals 0–5, 5–10, 10–20, 20–42, 42–80, and above 80 $\mu g/m^3$, respectively. The arrow on the horizontal axis indicates the location of the 42-$\mu g/m^3$ 1-h-average California air quality standard for H_2S. Also shown is the number of days per year with at least one breach of the 42-$\mu g/m^3$ level (top number) and the average length in hours of such episodes (bottom number).

SINGLE-SOURCE RESULTS

The grid size used in assessing regional impacts is too large to resolve individual plumes from each emission source. For this reason, we consider in this section the impact of a single source. The source is assumed to be an elevated Gaussian one with a height of 30 m and a standard deviation of 20 m in the horizontal direction and 10 m in the vertical direction. The results for all locations within the valley are very nearly the same, so only the results for one location will be presented.

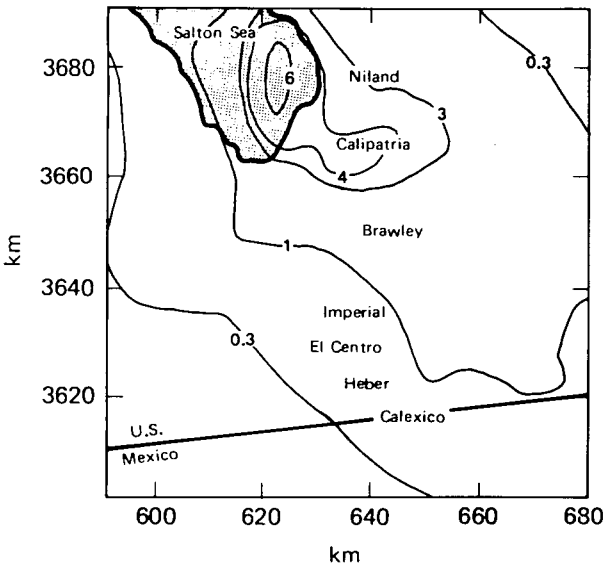

FIG. 13. Annual average ground-level SO_2 concentrations in $\mu g/m^3$.

In Fig. 14 the annual average concentration from a unit source (emission rate = 1 unit/s) is shown (in micro-units per cubic meter). The concentration for any source strength can be readily obtained by multiplying the contour level by the source strength. For example, if the source strength for a particular emission were 5 g/s, then all the contour levels in Fig. 14 would be multiplied by a factor of 5. Table 2 shows the factor by which each concentration contour should be multiplied in order to correspond to the emission levels used in this study. Noting that the peak concentration for the unit source is below 4 micro-units/m^3, it is readily seen that the maximum average concentrations of NH_3, Hg, and Rn are far below the federal standards.

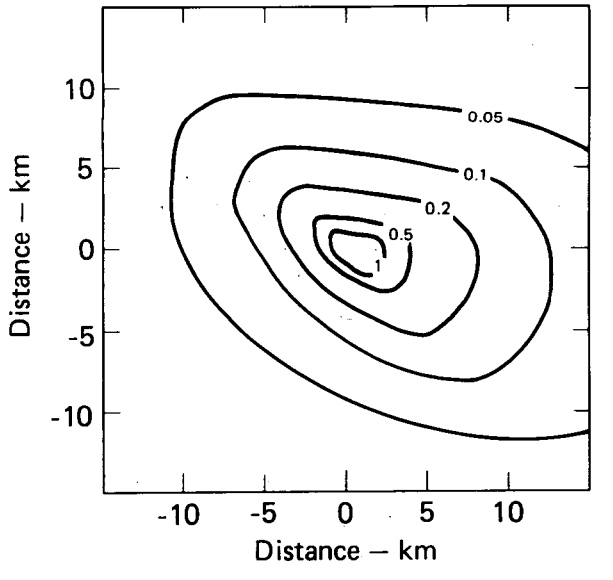

FIG. 14. Isopleth plot of the annual average ground level concentration in micro-units/m^3 for a unit source. The peak concentration is about 4 micro-units/m^3.

The situation is quite different, however, in the case of H_2S for which there is a 1-h standard. The peak ground-level concentration is predicted to occur within a distance of 1 km of the source, and this distance varies depending on atmospheric stability. At this distance and for the next few kilometers, the model calculations show the standard to be exceeded a significant amount of time. Taking the source as the center of a radial coordinate system, the probability of exceeding the 1-h standard as a function of radial distance can be calculated by integrating over the angular coordinate. This probability curve was calculated for both the 4.4 g/s source rate (Salton Sea and Brawley areas) and the 1.5 g/s source rate (Heber and East Mesa areas). It is shown in Fig. 15. The 4.4 g/s source rate resulted in violations of the standard out to a distance of 5 km, and the 1.5 g/s source rate resulted in violations out to a distance of 2 km.

A number of other calculations were made using different H_2S emission rates. These calculations indicate that if we are to keep violations of the H_2S standard within a 1-km radius of the source, the emission rate must be reduced to about 0.8 g/s. This corresponds to an emission rate of 30 g/MWh. Rule 455(b) in the Northern Sonoma County Air Pollution Control District (where The Geysers is located) restricts emissions to 50 g/ MWh by the year 1985.

TABLE 2. Emission factors for a 100-MW single source.

	Salton Sea and Brawley power plants, g/s	Heber and East Mesa power plants, g/s
H_2S	4.4	1.5
NH_3	49	13
CO_2	2400	3100.
Hg	0.0025	0.017
Rn	1200 [a]	1400 [a]

[a] The emission units for Rn are pCi/s.

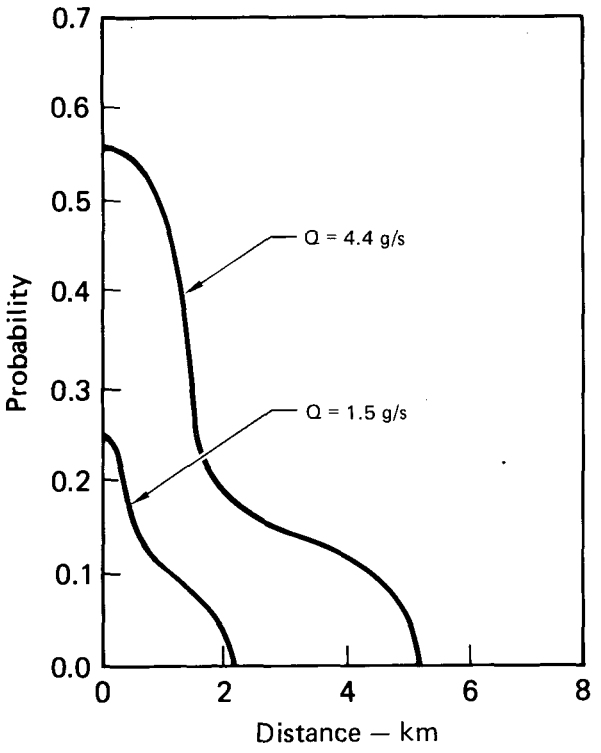

FIG. 15. The calculated probability of exceeding the 42 $\mu g/m^3$ one hour California air quality standard for H_2S as a function of radial distance from the source.

It might be noted that to keep the peak concentrations (as opposed to 1-h-average concentrations) below 42 $\mu g/m^3$ beyond 1 km, the emission rate must be reduced by another order of magnitude. It should also be noted that the peak concentrations near the source are highly dependent on the wind speed and occur when the wind speed is low. A small change in a low wind speed can result in a change in the concentration by a factor of two to three or more. Consequently, the calculated concentrations can vary considerably depending on the wind speeds used in the study. In addition, the resultant concentrations will depend highly on the height and size of the source as well as the source rate and meteorology. For these reasons, the calculated distances, beyond which the levels will not exceed the standard, are only approximations.

CONCLUSIONS

This assessment of the impact of a 3000-MW level of geothermal electrical energy production on air quality in the Imperial Valley, California has led to the following conclusions:

- The California 1-h standard for H_2S (42 $\mu g/m^3$) would be exceeded at ground level a significant amount of time over a large fraction of the valley. The standard would be violated at least 1% of the time over an area of approximately 1500 km^2 surrounding the power plants in the Salton Sea area and extending over the power plants in the Brawley area. Similar episodes would probably occur over areas of approximately 5 to 10 km^2 surrounding the clusters of power plants in the Heber and East Mesa areas.
- The northern cities in the valley would receive the highest H_2S exposure. The standard would be exceeded 10% of the time in Calipatria on about two-thirds of the days each year, and Niland and Brawley would experience similar violations 2% of the time on about 20% of the days each year. In the cities of Heber, Calexico, and Holtville in the southern part of the valley, the standard would be exceeded on about 4% (14 days) of the days each year, and in Mexicali, Mexico, a couple of days each year. No breaches of the H_2S standard are predicted for the central valley cities of El Centro and Imperial.
- Model calculations for a *single* power plant indicate that the H_2S standard is not exceeded beyond a distance of about 1 km when the emission rate is less than 0.8 g/s.
- The model predicts that nearly the entire valley—approximately 5000 km^2—would experience concentration levels in excess of 10 $\mu g/m^3$ (the average odor threshold) at least 1% of the time.
- The SO_2 standards would probably not be exceeded at the 3000-MW power level. At higher power levels, SO_2 standards would still not be exceeded as long as the H_2S standard were not exceeded. This assumes that H_2S is not converted

to SO_2 at the source and that the half-life of H_2S in the atmosphere is 13 h or greater.

- The levels of CO_2 produced by geothermal power plants would be within the normal fluctuations in the ambient concentration levels.
- The maximum ground-level concentrations of ammonia would be at least a factor of 10 below the federal standard.
- The maximum ground level concentrations of mercury would be at least a factor of 200 below the federal standard.
- The maximum ground level concentrations of radon and the short-lived radon daughter would be a factor of 10^5 below the federal standard.

These conclusions are based on the emission rates shown in Table 1 with no abatement.

ACKNOWLEDGMENTS

The authors appreciate the valuable support provided by numerous members of the Imperial Valley Environmental Project staff. We especially want to thank Michael Axelrod for his analysis of the meteorological and ambient air quality data, Vance Fowler for contributions made in the area of data base management, and Liena Boone for her computational support. We are indebted to David Layton for a critical review of the draft manuscript. Finally, the authors greatly appreciate the helpful comments and valuable guidance provided by Lynn Anspaugh and Paul Phelps during the entire conduct of the program.

REFERENCES

1. D.L. Ermak, R.A. Nyholm, and R. Lange, *ATMAS: A Three-Dimensional Atmospheric Transport Model to Treat Multiple Area Sources*, Lawrence Livermore Laboratory, Rept. UCRL-52603 (1978).
2. J.E. Welch, F.H. Harlow, J.P. Shannon, and B.J. Daly, *The MAC Method,* Los Alamos Scientific Laboratory, Los Alamos, New Mexico, Rept. LA-3425 (1965).
3. A.A. Amsden, *The Particle-In-Cell Method for the Calculation of the Dynamics of Compressible Fluids,* Los Alamos Scientific Laboratory, Los Alamos, New Mexico, Rept. LA-3466 (1966).
4. R.C. Sklarew, A.J. Fabrik, and J.E. Prager, *A Particle-In-Cell Method for Numerical Solutions of the Atmospheric Diffusion Equation, and Applications to Air Pollution Problems,* Systems, Science and Software, La Jolla, Calif., Rept. 3SR-844 (1971).
5. R. Lange, "ADPIC - A Three-Dimensional Particle-In-Cell Model for the Dispersal of Atmospheric Pollutants and Its Comparison to Regional Tracer Studies," *Appl. Meteor.* **17, 320-329 (1978).**
6. D.L. Ermak and R.A. Nyholm, *Multiple Source Dispersion Model,* Lawrence Livermore Laboratory, Rept. UCRL-52592 (1978).
7. P.H. Gudiksen, M.C. Axelrod, V.G. Fowler, K.C. Lamson, and R.A. Nyholm, *IVEP Baseline Air Quality and Meteorological Data,* Lawrence Livermore Laboratory Rept. (to be published).
8. P.H. Gudiksen, D.L. Ermak, K.C. Lamson, M.C. Axelrod, and R.A. Nyholm, *IVEP Air Quality Study,* Lawrence Livermore Laboratory Rept. (to be published).
9. J.L. Renner, D.E. White, and D.L. Williams, "Hydrothermal Convection Systems," in *Assessment of Geothermal Resources of the United States,* U.S. Geological Survey, Circ. 726 (1975).
10. D. Towse, *An Estimate of the Geothermal Energy Resource in the Salton Trough, California,* Lawrence Livermore Laboratory, Rept. UCRL-51851 (1975).
11. D.L. Ermak, "A Scenario for Geothermal Electric Power Development in Imperial Valley," *Energy* 3, 203-217 (1978).
12. D.E. Robertson, J.S. Fruchter, J.D. Ludwick, C.L. Wilkerson, E.A. Crecelius, and J.C. Evans, "Chemical Characterization of Gases and Volatile Heavy Metals in Geothermal Effluents," Geothermal Resources Council, TRANSACTIONS **2,** 579 (July 1978).
13. H.S. Pines and M.A. Green, *The Use of Program GEOTHM to Design and Optimize Geothermal Power Plant Cycles,* Lawrence Berkeley Laboratory, Berkeley, California, Rept. LBL-4454 (1976).
14. M. Walker, Republic Geothermal, private communications (1978).
15. W. Smith, Union Oil Company, private communication (1978).
16. M. Carroll, San Diego Gas & Electric Co., private communication (1978).
17. D.F. Adams, F.A. Young, and R.A. Huhr, "Evaluation of an Odor Perception Threshold Test Facility," *Tappi* **51,** 62A-67A (1968).

SKM/gw

APPENDIX A. IMPACTS OF OTHER SCENARIOS

The impact of emissions from geothermal power plants on the concentration of gaseous substances in the air throughout California's Imperial Valley will depend on several factors: the emission rate (which, in turn, is a function of the content in the geothermal fluid, the chemical and physical properties of the geothermal fluid, and the efficiency of conversion and abatement technologies), the size and location of individual power plants, and the total number of power plants throughout the valley. There is considerable uncertainty in all of these factors since geothermal development in the Imperial Valley is only in the initial stages.

A principal uncertainty is the emission rate. Initial source concentration measurements have varied over an order of magnitude. This is typical of geothermal fluids, even those obtained from wells within the same KGRA. In addition, the fractional content of the fluid is generally found to vary with time. Consequently, greater confidence in the emission rate estimate can be gained only as more wells are drilled and continually monitored. The maximum level of power production in the valley will also become more precisely known as the experience of developers leads to a better understanding of the geothermal resource and our ability to exploit it.

The analysis in this appendix is intended to provide a means of estimating the regional air quality impacts of geothermal development, should emission rates be found to vary considerably from those assumed in this study. The scenario treated here includes five emission sources in each KGRA and treats each cluster of 5 sources separately. Each of the five emission sources had a unit (1 g/s) emission rate for a total emission rate of 5 g/s. The source height and size are the same as those used in the other sections of this report. The annual average concentration from each cluster of sources has been calculated, and the results can be combined with the proper weighting to estimate the impact from a variety of scenarios with different emission rates and total capacity per KGRA.

Contour plots of the annual average concentration levels for each cluster of sources are presented in Fig. A-1. The concentration levels are in $\mu g/m^3$. The concentration levels are seen to be somewhat higher in the northern part of the valley. The peak concentration in the Salton Sea and Brawley areas is about 30 $\mu g/m^3$, while the peak level in the Heber and East Mesa areas is about 10 $\mu g/m^3$. The differences in the concentration levels are due solely to the different meteorology in the different locations.

As an example of how these results can be combined, the Salton Sea and Brawley contour levels have been combined using a weighting factor of 1, and the result is shown in Fig. A-2. In this scenario, there are equal emissions from the cluster of power plants in the Salton Sea and Brawley areas and none from the Heber and East Mesa areas. Combining these concentration levels with those from the cluster of sources in the Heber and East Mesa area, again using a weighting of 1, produces a scenario where there are equal emissions from each of the four clusters of sources. The contour plot for this scenario is shown in Fig. A-3. The appropriate weighting factor for each contour level is obtained by multiplying the contour level value in the figure by the emission rate (g/s) per power plant (assuming there are 5 power plants in each cluster) or by multiplying the contour level value in the figure by 1/5 the emission rate (g/s) per power plant cluster. In this way, the results shown in Fig. A-3 can be used to predict the impact of a 2000-MW scenario, with 500 MW produced in each KGRA and with equal emission rates per KGRA.

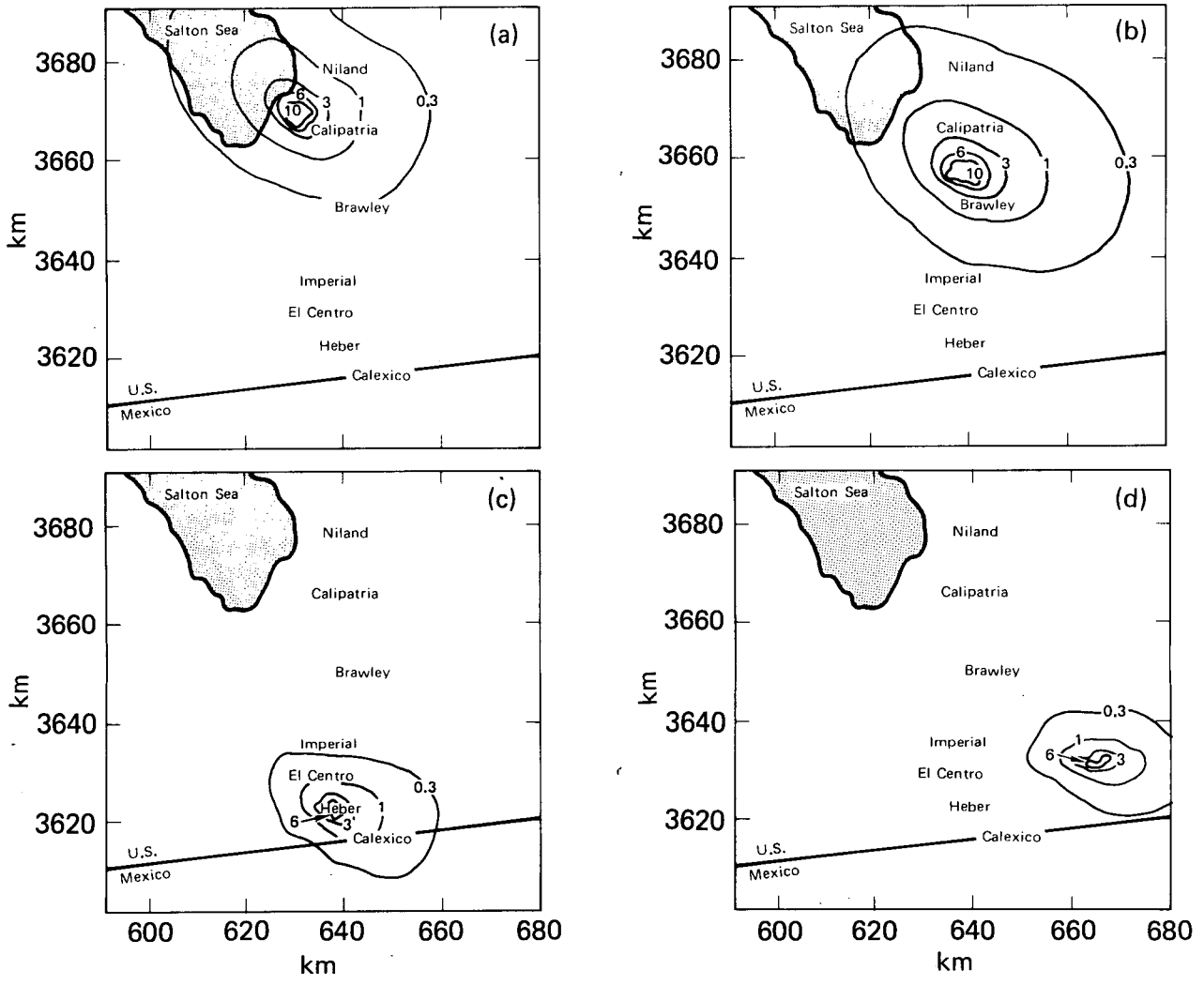

FIG. A-1. Isopleth plot of the annual average ground level concentration in $\mu g/m^3$ for five unit sources located in (a) the Salton Sea KGRA, (b) the Brawley KGRA, (c) the Heber KGRA, and (d) the East Mesa KGRA.

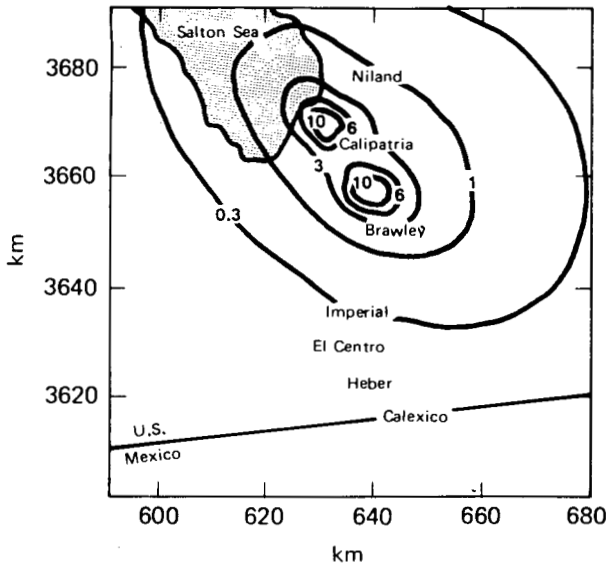

FIG. A-2. Isopleth plot of the annual average ground level concentration in $\mu g/m^3$ for five unit sources located in the Salton Sea KGRA and five others in the Brawley KGRA.

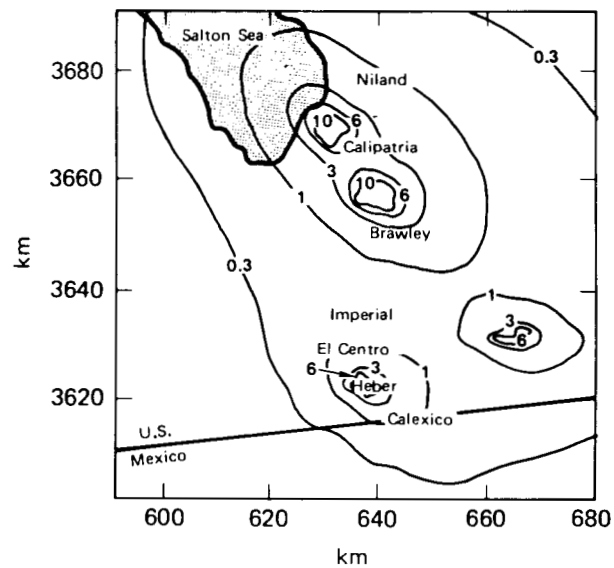

FIG. A-3. Isopleth plot of the annual average ground-level concentration in $\mu g/m^3$ for five unit sources located in each of the following KGRAs: Salton Sea, Brawley, Heber, and East Mesa.

*LLL: 1979/6